Journal of Mechanical Engineering and Sciences (JMES)
ISSN (Print): 2289-4659; e-ISSN: 2231-8380
Volume 10, Issue 2, pp. 2084-2097, September 2016

DOI: https://doi.org/10.15282/jmes.10.2.2016.13.0197

Effect of material discontinuity on the flanges of axially compressed cylinder

O. Ifayefunmi * and Lu Kian Hap

Faculty of Engineering Technology
Universiti Teknikal Malaysia Melaka (UTeM),
76100 Durian Tunggal, Melaka, Malaysia
*Email: olawale@utem.edu.my
Phone: +6062346408; Fax: +6062346526

ABSTRACT

The aim of this paper was to examine the buckling behavior of axially compressed mild steel circular cylinder with introduced local material discontinuity on the flange of a percentage of the hoop length of the cylinder. The work was both experimental and numerical. The cylinders were made from welded mild steel plate and they had integral top and bottom with 10 mm thick flanges in them. The flange was fully welded to one end of the cylinder. Meanwhile, at the other end of the cylinder, material discontinuity was introduced. Five laboratory scaled cylinders were manufactured with nominal geometry given by R/t = 25.0, L/R = 2.24 and wall thickness, t = 2.0 mm. Numerical results were obtained using the ABAQUS finite element code. Results of the experimental tests and the accompanying numerical calculations of the load carrying capacity of the cylinders were provided with a special attention devoted to the effect of material discontinuity along the flange on the buckling behavior. There was a good agreement between the test data and the numerical predictions [(206.6 kN, 211.66 kN), (205.99 kN, 211.67 kN), (206.87 kN, 212.72 kN), (207.16 kN, 210.63 kN), (207.49 kN, 210.71 kN)]. It can be concluded that for an axially compressed cylinder with R/t = 25.0, the effect of material discontinuity on the flange on the buckling load of the cylinder was insignificant**.**

Keywords: Axial compression; buckling; cylinder; material discontinuity.

INTRODUCTION

Thick cylindrical shells find application mainly in pressure vessels, marine and offshore industries, especially for onshore and offshore pipelines. Their primary purpose is to transport petroleum products from one location to the other. When they are used for onshore/offshore pipelines, they covered a wide range of distance which could span over thousands of kilometers. However, for the ease of installation purposes, it is more convinient to machine/manufacture this cylindrical pipeline in transportable pieces and then join them together on the sites. To join the cylinders together, one of the most common method is the use of flanges. However, during the welding process of such cylinders with integral flanges, due to the different quantities of heat input as well as the quality of the weldments, many problems arise from the process [1, 2]. There are the possibilities of material discontinuity/crack of a percentage of the circumference of the cylinder as a result of this problem. The presence of material discontinuity/crack in pressure vessel components always places the structural integrity at risk of failure [3].

Then, a valid question arises on what would happen to the load carrying capacity of such cylinders with material discontinuity along the flanges.

In the last few decades, many researchers in shell buckling had devoted some attention to the imperfect sensitivity of such shell structure subjected to various loading conditions [4]. In fact, several research work had been carried out on the effect of crack on the buckling behavior of isotropic and composite cylinders having through cracks with varying crack lengths and crack orientations (i.e., longitudinal, circumferential and angled) on the cylindrical specimen. Estekanchi and Vafai [5], proposed and developed finite element models by employing the meshing scheme for cracked cylinders with various through crack lengths and orientations. Buckling behavior of titanium cylindrical shell with an initial through crack on the cylinder under compressive loading had been researched into using the numerical approach [6]. In [7, 8], numerical analyses into the effects of axial and circumferential through cracks along the cylinder on the buckling behavior of aluminum cylindrical shells under single loading were presented. A similar analysis was carried out for aluminum cylinders with through crack (axial, circumferential and angled) subjected to combined loading [8-13]. Shariati et al. [14] conducted linear and non-linear analyses of finite element analysis using ABAQUS to investigate the effects of crack position, crack orientation and crack length on the buckling and post-buckling behavior of thick and long cracked steel cylindrical shells subjected to combined loading. The finite element results were benchmarked by conducting several experimental buckling tests. Analytical and experimental studies of the non-linear response of the buckling behavior of aluminum cylinder with long longitudinal crack were presented in [15, 16]. Results were presented for internal pressure, axial compression load and combined internal pressure and axial compression. Research into the effect of buckling behavior of cylinder with crack is not limited to isotropic cylinder alone. This idea has been explored for cracked composite cylindrical shells subjected to axial compression [17-19] and to combined loading [20, 21]. However, from the literature, there was no work found on the buckling behavior of cylinder with crack along the flanges. In addition, except for the work done by Refs [14-16], where numerical/analytical results were benchmarked by conducting several experimental buckling tests, all other works centered on theoretical/numerical work only. The present work concentrated on the effect of material discontinuity or crack along the flange of welded mild steel cylinder on its load carrying capacity when subjected to axial compression. In the present study, five laboratory scaled mild steel cylinder were tested and the results were benchmarked using the general purpose finite element code ABAQUS.

METHODS AND MATERIALS

Cylindrical Model Geometry

Five cylindrical models, CY1, CY2, CY3, CY4 and CY5 were manufactured from 2 mm flat mild steel plate. Cylinders were assumed to have the following nominal geometry: Diameter, D = 100 mm, axial length, L = 112 mm and uniform wall thickness, t = 2.0 mm. The models were manufactured with welded top and bottom of 10 mm thick flanges as shown in Figure 1. Circumferential crack of different lengths were introduced on the flanges of the specimens during the manufacturing process. Cylinders were joined together using the Metal Inert Gas (MIG) welding process. All cylinders were subjected to axial compression. The effect of flanges on the buckling behavior of axially compressed perfect cylinder with no material discontinuity was

examined. It was decided to test a cylinder with welded flange and compare the buckling load to a circular cylinder without a flange. Figure 1 shows the photograph of both cylinders, Figure 1(b) with flanges and Figure 1(c) without flanges. Both cylinders were subjected to axial compression using a universal INSTRON machine at a loading rate of 1 mm/min. Figure 2 depicts the plot of load against axial shortening for both axially compressed cylinders, i.e., one with flanges and the other without flanges. It can be seen that both cylinders produced plots that were in close agreement (nearly identical). Also, the magnitude of the collapse load for both cases were in very good agreement with about 1% difference (206.6 kN vs 208.56 kN) for the cylinder with flanges and the cylinder without flanges respectively.

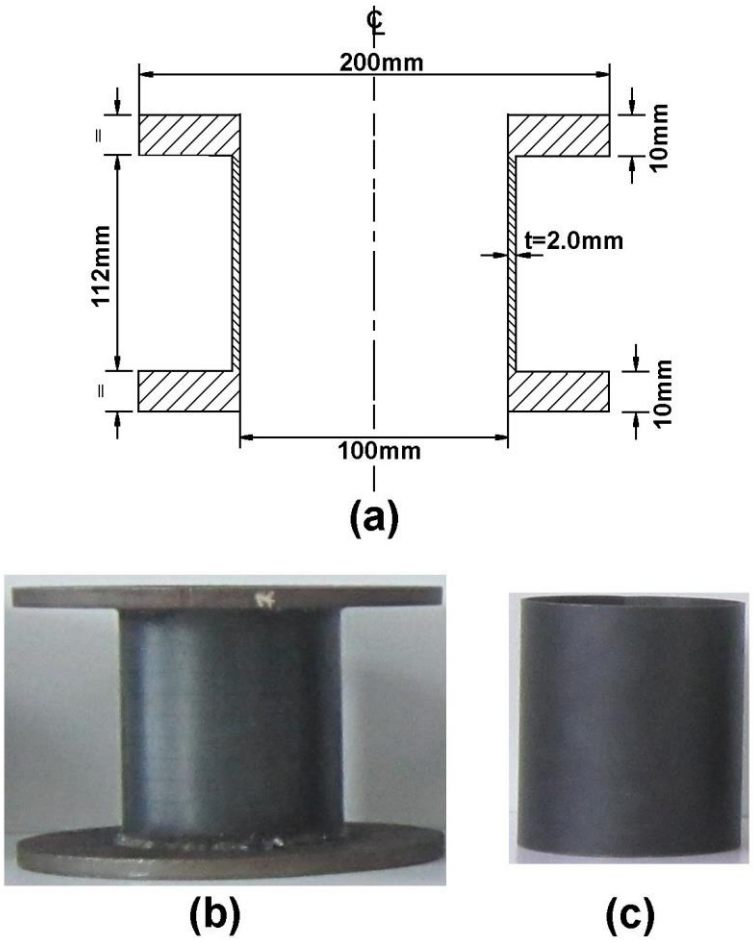

Figure 1. Cylindrical specimen geometry (a) section through cylindrical shell; (b) welded cylinder with flanges; (c) welded cylinder without flanges.

In addition, it can be observed that both cylinder faileds through the excessive plastic straining at one end of the cylinder as shown in Figure 3. Hence, it was apparent that the effect of flanges on the buckling behavior of axially compressed cylinder with no material discontinuity was less significant, i.e., the introduction of flanges did not affect the load carrying capacity of the cylinder when subjected to axial compression. This can be attributed to stress concentration on the cylindrical specimen rather than on the flange because the thickness of the flange (10 mm) was relatively large with respect to the cylindrical specimen thickness of 2 mm [22].

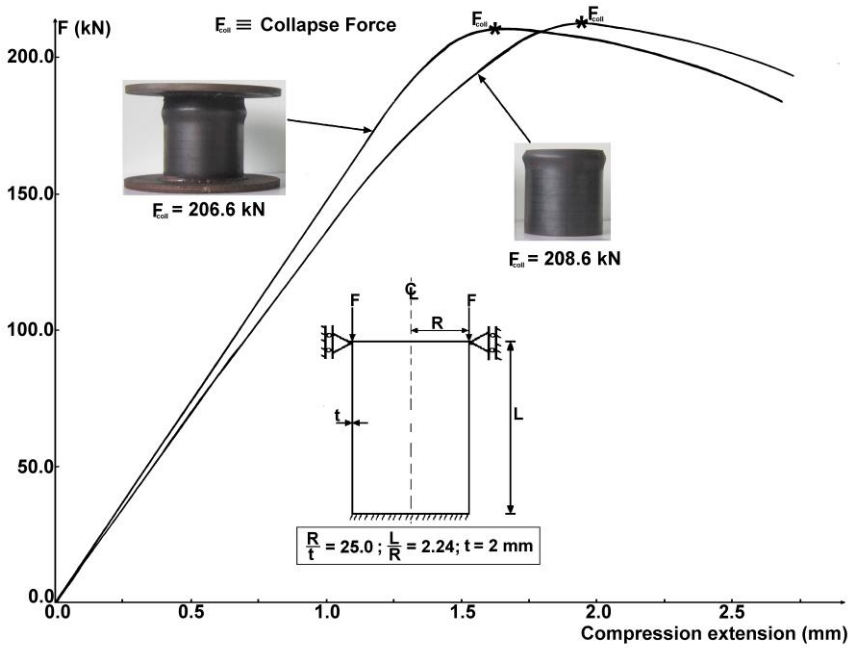

Figure 2. Plot of load versus compression extension for axially compressed cylinder, one with flanges and the other without flanges.

Figure 3. The collapse cylinders bulging out in the neighborhood of one end of the cylinder.

Experimental Procedure

This section presents the experimental procedure into the effect of material discontinuity on the flanges of the cylinder on the magnitude of its load carrying capacity when subjected to axial compression. Details about the material properties extraction, the specimen manufacturing processes, pre-test measurement and collapse test are described. The material properties of 2 mm mild steel plate were obtained by testing three flat tensile specimens under a uni-axial tensile test using the INSTRON testing machine. The tensile specimens were machined according to the British Standard BS EN 10002-1:2001 [23]. All tensile specimens were tested until they failed with an extensometer for calculating the values of strain. The speed rate of loading was 1.0 mm/min. Cylindrical specimens CY1, CY2, CY3, CY4 and CY5 were manufactured

using several manufacturing processes. Initially, cylindrical specimens were cut and rolled from a flat mild steel plate. Next, the ends of the rolled specimens were joined together using the MIG welding process. Then, the flanges were welded to the circular cylinder as shown in Figure 4. During the welding process, the flanges were fully welded to one end of the cylinder. While at the other end of the cylinder, material discontinuity/circumferential cracks of varying lengths were introduced on the specimens. The magnitude of the circumferential crack, 2a, to the cylinder circumference, $2a/2\pi R$, was varied between 0.0 to 0.25. Circumferential crack lengths introduced on specimen model CY2, CY3, CY4 and CY5 were 0.05, 0.1, 0.2 and 0.25 respectively, as exemplified in Figure 5 for the cylinder with cracks extending over 0.25% of the circumference (CY5). Meanwhile, cylindrical model CY1 was assumed to be a nearly perfect model. However, it must be mentioned that both the flat tensile specimens and the cylinders were not stress relieved at any point during and after the manufacturing process. All cylinders were to be subjected to axial compression.

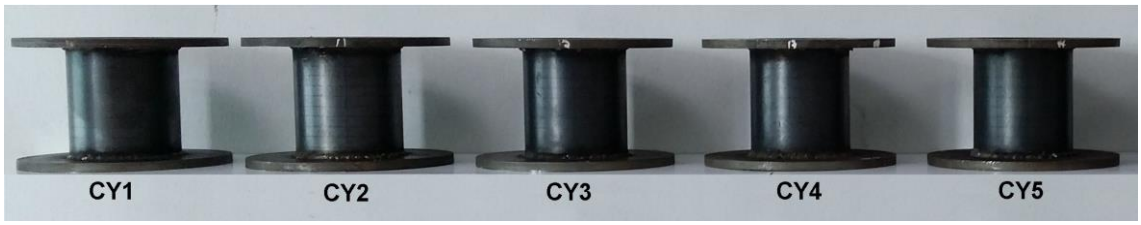

Figure 4. Photograph of MIG welding cylinders with top and bottom flanges.

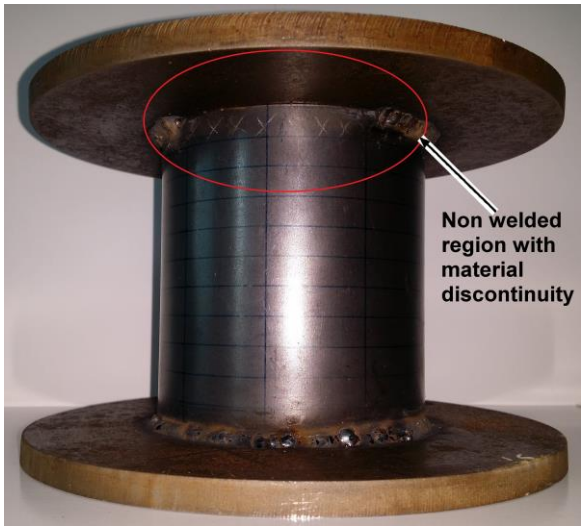

Figure 5. Cylinder CY5 with introduced circumferential material discontinuity on the top flange.

Prior to testing, a number of measurements were taken on all cylindrical specimens. First, the wall thickness was measured using an Ultrasonic thickness measurement gauge at eleven different equidistance points along the axial length of the cylinder. This was then repeated along 36 deg spaced along the circumference of the cylinder, resulting in 11 by 10 = 110 measuring points. The average t_{ave}, minimum t_{min} and maximum t_{max} wall thickness for all specimens are provided in Table 1. It can be seen that cylindrical model CY2 had the lowest amount of data variation, while

cylindrical model CY4, had the highest amount of dispersion from the set of measured wall thicknesses for the cylinders. Then, both the inner and outer diameters of the cylinders were measured at five equally spaced diameters using a digital Vernier caliper at the top and bottom ends respectively. The average mid-surface diameter at the top and bottom for all cylinders are given in Table 2. The average mid-surface diameter was assumed to be the sum of the average inner diameter of the cylinder and the average wall thickness of the cylinder (i.e., $\overline{D} = D_{inner} + t$). Finally, the axial lengths of all cylinders were measured using the digital Vernier caliper. The corresponding average values and standard deviation of axial length for all cylinders are also presented in Table 2. Again, it was apparent that cylindrical model CY2 had the lowest deviation, while cylindrical CY4 had the highest variation of the measured data.

Table 1. Measured values of the wall thicknesses for all tested cylinders.

	t_{nom}	t_{min}	t_{max}	t_{ave}	t_{std}
			(mm)		
CY1	2.0	2.02	2.12	2.05	0.02856
CY2	2.0	1.98	2.08	2.05	0.01746
CY3	2.0	1.96	2.10	2.06	0.01913
CY4	2.0	1.94	2.09	2.04	0.02877
CY5	2.0	1.97	2.11	2.06	0.02425

Table 2. Measured data of diamters and axial length for all tested cylinders. Note: $\overline{D}$ ≡ average mid-surface diameter.

	$\overline{D_{top}}$	$\overline{D_{bottom}}$	L_{ave}	L_{std}	$\overline{D_{top}}/t_{ave}$	$L_{ave}/\overline{D_{top}}$
			(mm)			
CY1	101.95	102.04	111.06	0.0295	49.73	1.089
CY2	101.98	101.96	110.98	0.0227	49.75	1.088
CY3	101.66	101.96	111.05	0.0382	49.35	1.092
CY4	102.03	101.96	111.1	0.0433	50.01	1.089
CY5	102.04	102.06	111.03	0.0369	49.53	1.088

Finally, all cylindrical specimens (CY1, CY2, CY3, CY4 and CY5) were subjected to axial compression using the Universal Instron 8802 Machine. The specimen was placed between the platens of 250 kN INSTRON machine. It was assumed that the platen of the INSTRON machine will help to provide the same boundary condition used in the numerical simulation approach section, i.e., the cylinder was fixed at one end, i.e., $u_x = u_y = u_z = \Phi_x = \Phi_y = \Phi_z = 0$. The same boundary condition was applied at the other end except for $u_z \neq 0$. Incremental axial load was applied to one end of the cylindrical specimen at the rate of 1.0 mm/min. This was the same rate of loading used to obtain the material properties of the mild steel plate from which the cylinders were made.

Numerical Model Simulations Approach

In this section, an appropriate finite element model was developed for the problem statement in order to validate the experimental results. From the previous sub-section, it

was evident that there was no difference between the load carrying capacity of cylinder with or without flanges, i.e., the effect of flanges on the buckling behavior of axially compressed cylinder was insignificant. Then, for the finite element modeling, it was decided to model the cylinder as sketched in Figure 6(a). The cylinders were assumed to be subjected to axial compression (Figure 6(b)).

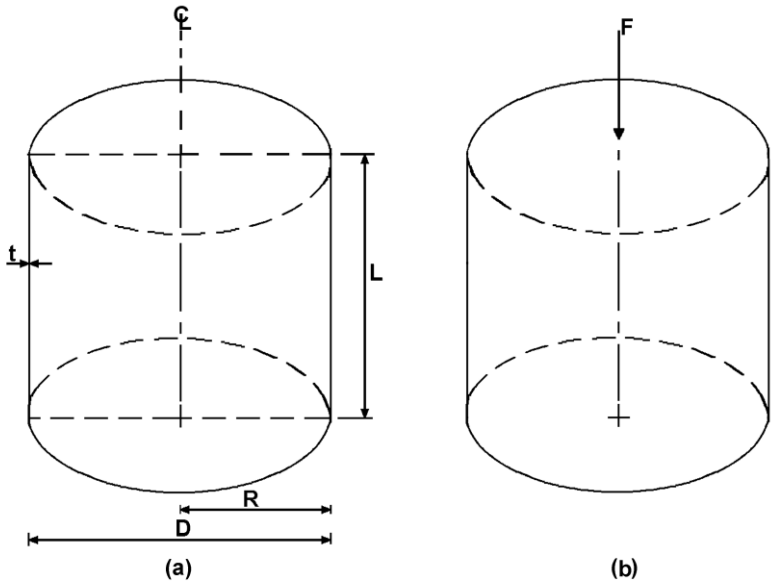

Figure 6. (a) Geometry of analysed cylinder; (b) subjected to axial compression.

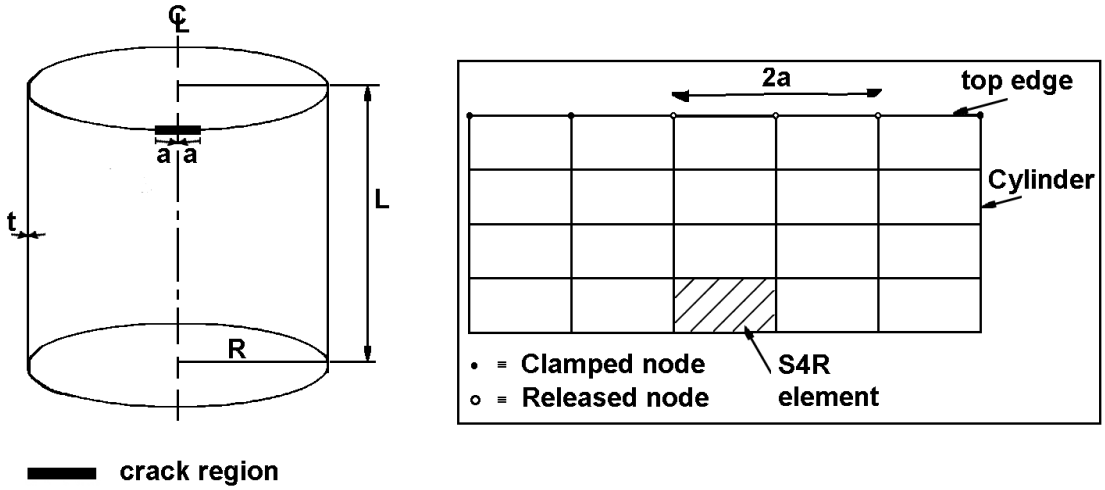

Figure 7. Illustration of the location of material discontinuity over the limited hoop length of the cylinder top flange.

Assume that the Finite element models were given by the radius-to-thickness ratio, R/t = 25.0, 50.0, 100.0, and nominal thickness, t = 2.0 mm, 1.0 mm, 0.5 mm, respectively. The length-to-radius ratio will remain constant for all cylinders, L/R = 2.24. It was assumed that the cylinders had local material discontinuities at the flanges such as crack over the limited hoop length as illustrated in Figure 7. The material discontinuity was located at the end of the cylinder where the axial load was applied. The specimens were modeled using the four-node three-dimensional doubly curved

shell elements with six degrees of freedom (S4R). Non-linear static analysis was carried out using the modified Riks method algorithm, which was implemented in ABAQUS. The cylinder was assumed to be fully clamped at one end, i.e., displacement and rotation degree of freedom were constrained in all direction ($u_x = u_y = u_z = \Phi_x = \Phi_y = \Phi_z = 0$). Meanwhile, at the other end (point of load application), the cylinder was only allowed to move in the axial direction, i.e., the same boundary conditions were applied except for $u_z \neq 0$. The notation used above assumed: u ≡ displacements, and Φ ≡ rotations.

RESULTS AND DISCUSSION

Experimental Results

The summary of the material properties data which were obtained from the uni-axial tests for all specimens is presented in Table 3. Figure 8 depicts a typical stress-stress curve (for tensile specimen 3). It is seen here that the stress-strain curve was linear up to the yield stress, i.e., the elastic region, where stress was directly proportional to the strain. The post-elastic region showed the yielding region where the material started to deform plastically. The specimens kept its deformed shape even if the load was removed, leading to plastic deformation. As a result of plastic deformation, strain hardening region was reached i.e., a region on the curve where the material began to strengthen itself against the applied load. The material strain hardening continued up to the ultimate tensile strength (UTS) of the material. At the point of UTS, necking/constriction of the material began to form, i.e., cross section area of the material began to decrease in a localized region, until the material failed at the point of necking.

Table 3. Set of material data obtained from uni-axial tensile tests on mild steel plate (E = Young's modulus, UTS = ultimate tensile strength).

Specimen pecimen	E (GPa)	Upper yield (MPa)	Lower yield (MPa)	UTS (MPa)
1	256.2	311.7	289.2	363.6
2	227.3	322.8	312.4	384.0
3	240.8	331.9	287.9	375.6
Average	241.4	322.1	296.5	374.4

Table 4. Comparison of experimental and numerical results. Numerical results were based on ABAQUS FE code, and on average geometry given in Table 2. Note: 2a/2πR ≡ magnitude of circumferential crack to the cylinder circumference.

Specimens	2a/2πR	Collapse Force (kN)		Numerical/Exptl.
		Experimental	Numerical	
CY1	0.0	206.60	211.66	1.0245
CY2	0.05	205.99	211.67	1.0276
CY3	0.1	206.87	212.72	1.0283
CY4	0.2	207.16	210.63	1.0168
CY5	0.25	207.49	210.71	1.0155

The compression extension and the corresponding load at each increment were measured by the machine, as depicted in Figure 2, for the cylinder with no crack. Figure 9 shows the deformed shape for all cylindrical specimens after testing and the corresponding collapse loads are given in Table 4. It can be noticed from Figure 9 that all cylinders had a similar failure pattern, i.e., axisymmetric bulging at one end of the cylinder at almost the same height along the meridian. In addittion, it was apparent from Table 4 that cylindrical model CY2 had the lowest collapse force which was consistent and in agreement with the thickness variation of the specimens as seen in Table 1, where cylindrical model CY2 had the lowest thickness variation.

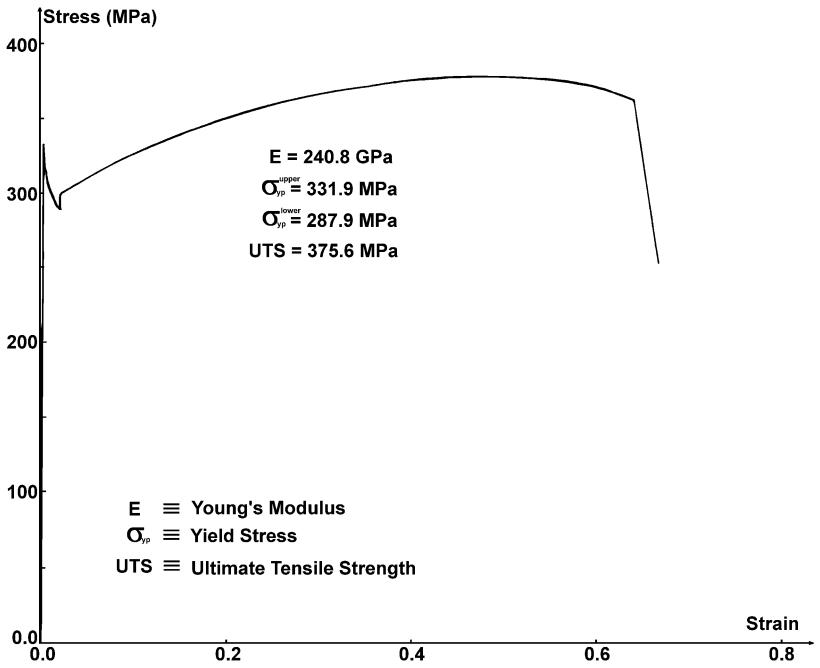

Figure 8. Typical stress strain plot for 2 mm thick mild steel tensile specimen 3.

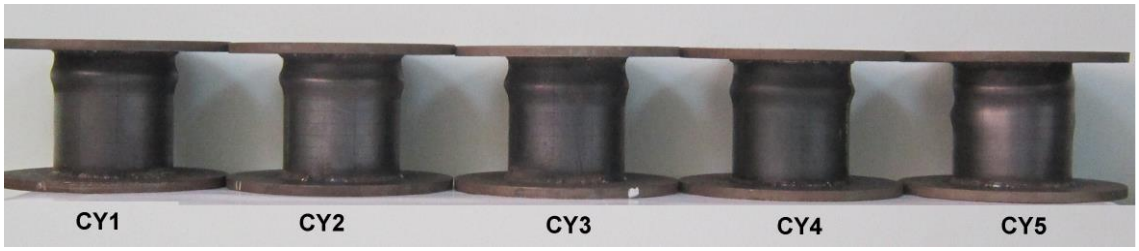

Figure 9. Photograph of cylinder with flanges after testing.

Numerical Predictions

Numerical results of the buckling behavior analysis of circular cylinder with the range of radius-to-thickness (R/t) ratios ranging from 25.0 to 100.0 and subjected to axial compressive loading are presented in this section. The cylinders were assumed to be made from mild steel and the materials were modeled as elastic and perfectly plastic using the average values of material data presented in Table 1, i.e., Young's Modulus, E = 241.4 GPa, Yield Stress, σ_{yp} = 322.1 MPa and Poissons ratio, υ = 0.3. Figure 10 depicts a typical plot of load against axial shortening for the axially compressed perfect cylinder with different radius-to-thickness ratios, R/t. It was apparent from Figure 10,

that the resulting load-deflection curves were nearly linear up to the collapse load. The post-collapse path showed that there was a gentle fall in the load carrying capacity of the cylinder. However, reducing the radius-to-thickness ratio increased the cylindrical shell's resistance to deformation.

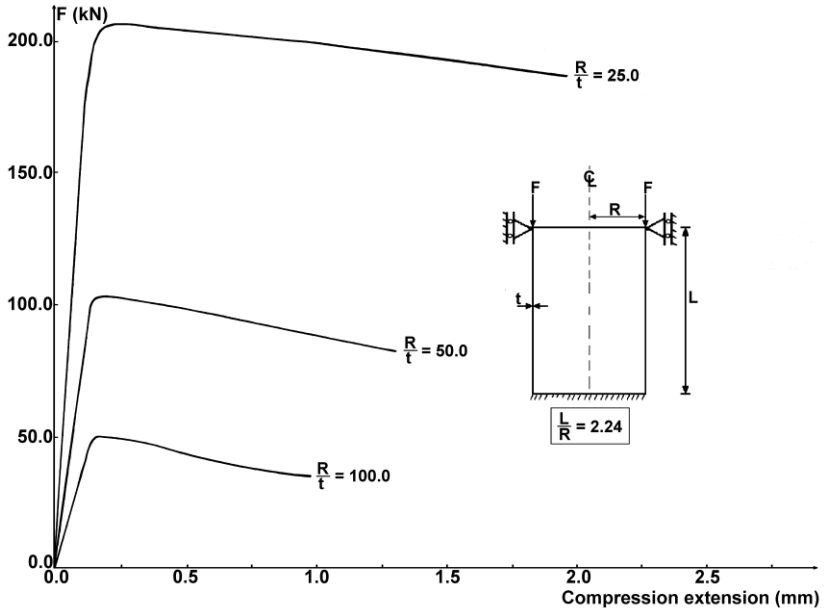

Figure 10. Numerical simulation plot of load against compression extension for perfect cylinder with different radius-to-thickness ratio subjected to axial compression.

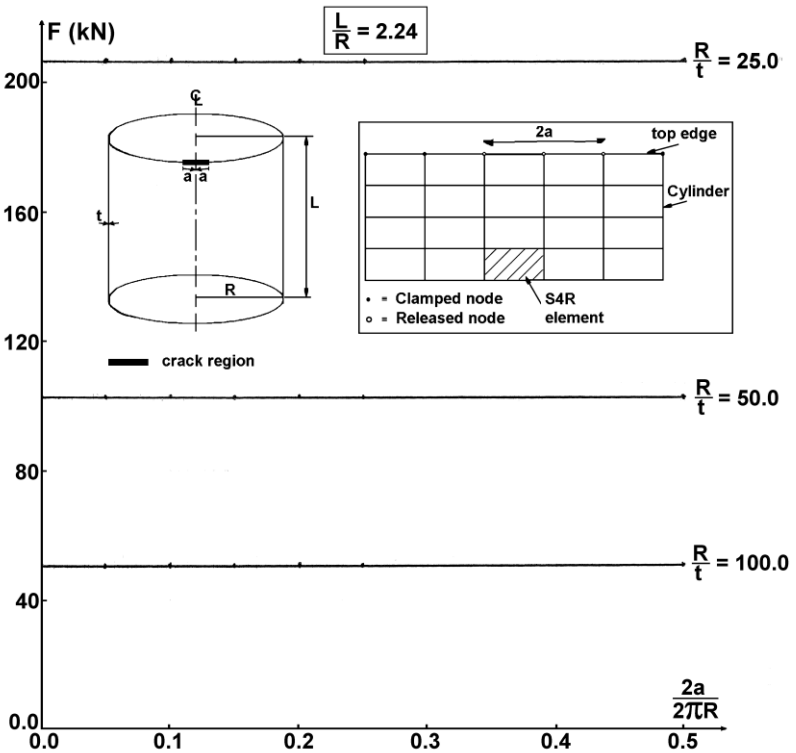

Figure 11. Numerical prediction of the effect of material discontinuities (crack) on the flanges of axially compressed cylinder on its buckling strength for different radius-to-thickness ratios.

Figure 11 presents the plot of buckling load corresponding to different imperfect models having a crack against the increasing length of crack for the cylinder with different radius-to-thickness ratios, R/t. It was apparent that the presence of circumferential crack on the flanges of the cylinder did not have any significant effect on the reduction of the load carrying capacity of the cylinder for all the radius-to-thickness ratios considered. This can be attributed to the fact that when the cylinder was loaded, the two edges of the crack sat on each other and the cylinder tended to behave in a similar manner to a perfect (non cracked) cylindrical shell [14].

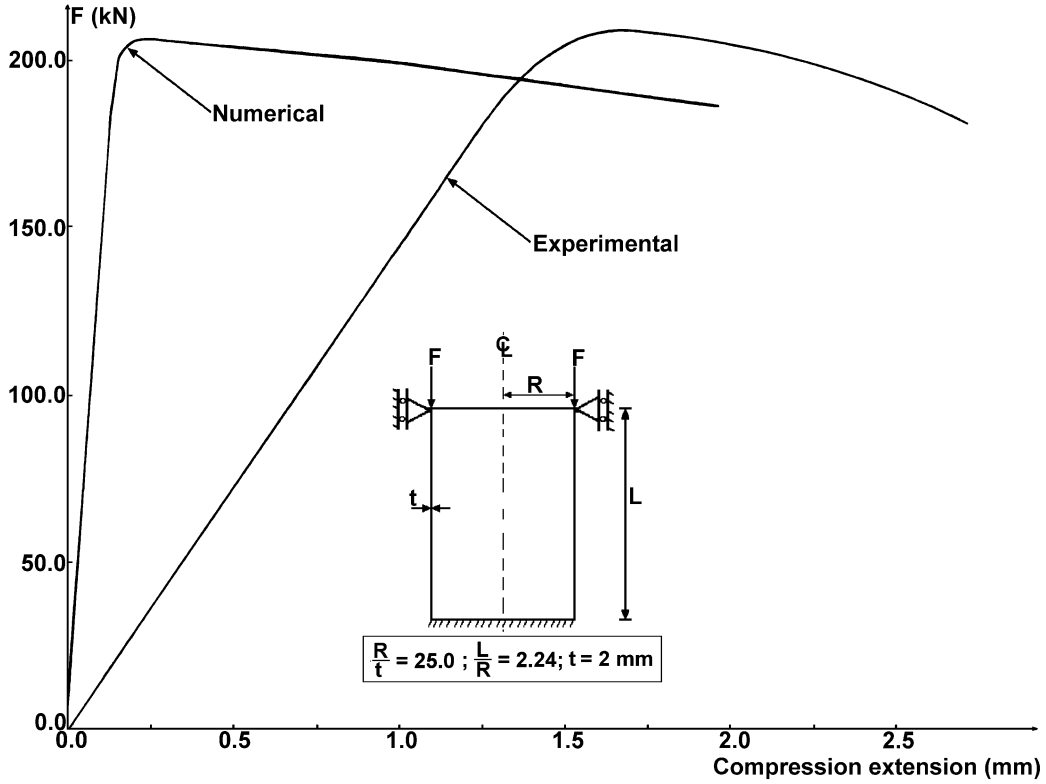

Figure 12. Comparison of experimental and numerical plots of load versus compression extension for axially compressed cylinder (no crack) with, R/t = 25.0. Note: Numerical result was obtained using nominal wall thickness, t = 2 mm.

Comparison of Experimental and Numerical Results

The results of experiments were compared with the numerical predicted results. Figure 12 depicts the plot of axial force against compression extension for both experimental and numerical predictions for cylinder without material discontinuity. Both plots followed a similar path i.e., the load deflection curve was nearly linear up to the collapse load. The first linear stage before the first yield force was when the structure deformed elastically. The next stage, just above the first yield force, was the transition stage when plastic deformation arose and extended through the wall thickness of the shell and along its length. It can be seen here that the FE predictions of the slope underestimated the experimental values. Comparisons between the experimental collapse forces and the numerically predicted collapse forces for all cylinders based on the average measured geometry are given in Table 4. It was apparent from Table 4, that there was a marginal difference between the experimental and numerical results. For

example, the highest discrepancy between the ratio of numerical prediction to the experimental result was 2.83% (i.e., 206.87 kN vs 212.72 kN). The goodness of the results can be attributed to: (i) the use of exact material properties from which the specimens were made from during numerical simulation, and (ii) adoption of the same end support at both sides of the cylinder during experimentation and numerical calculations [24].

Figure 13 presents the plot of buckling load corresponding to different imperfect models having a crack against the increasing length of crack. It can be observed again from Figure 13 that both plots showed a similar trend, i.e., increasing the circumferential crack length along the flange of the cylinder did not affect the magnitude of the buckling strength of the cylinder when subjected to axial compressive loading. Again, this was also consistent with the experiemental data presented in Table 4. This may not be generally true for all other geometry, since past results had revealed that for conical shell, material discontinuty along the flange of small radius ends of the cone will have a significant effect [25, 26]. Hence, there is need for more research work in this area.

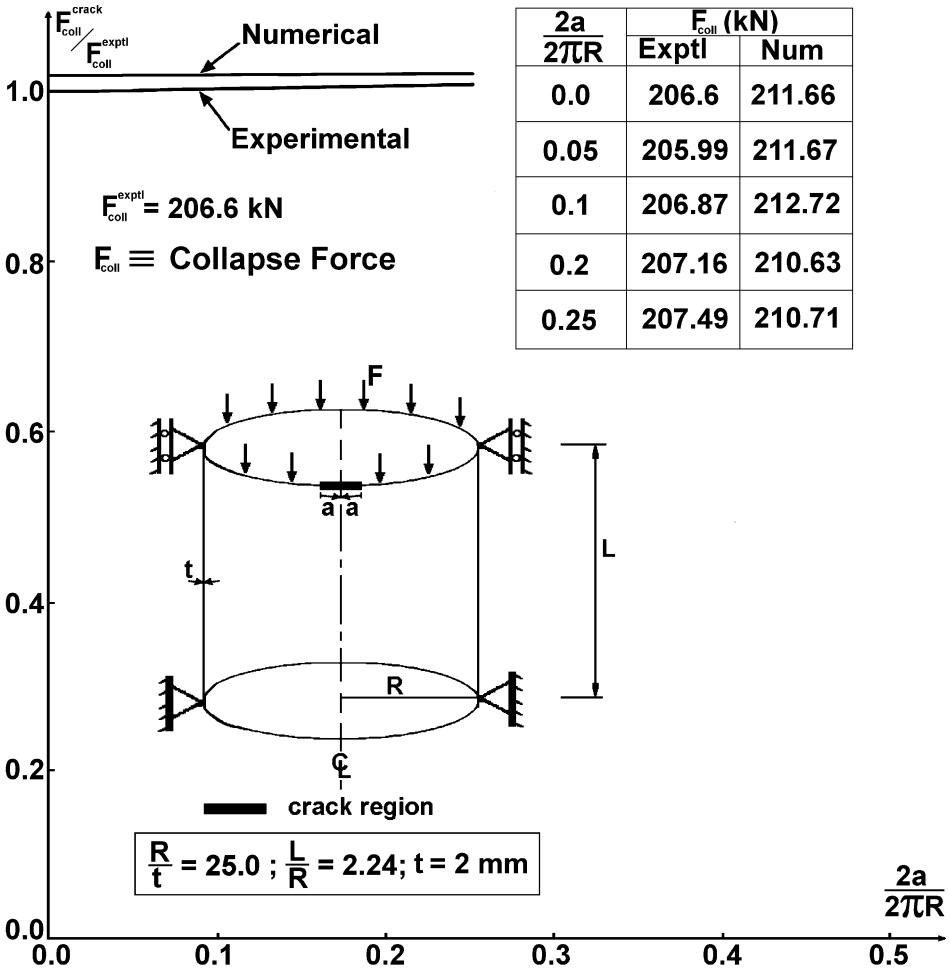

$\frac{2a}{2\pi R}$	F_{coll} (kN)	
	Exptl	Num
0.0	206.6	211.66
0.05	205.99	211.67
0.1	206.87	212.72
0.2	207.16	210.63
0.25	207.49	210.71

Figure 13. The effect of material discontinuities (crack) on the buckling strength of axially compressed cylinder. Comparison of experimental and numerical results for cylinder with, R/t = 25.0.

CONCLUSIONS

Comparison of experimental data and numerical prediction into the buckling behavior of circular cylinder with material discontinuity/circumferential crack along the welded flange subjected to axial load revealed that there was a good agreement between the test data and the numerical predictions. Based on the predictions from both results, two main assumptions can be inferred, and they were: (i) the magnitude of circumferential crack length along the flange of the circular short mild steel cylinder with radius-to-thickness ratio ranging from 25.0 to 100.0, did not affect the buckling strength of the cylinder under axial compression, and (ii) it had been shown that the introduction of flanges on a relatively thick short mild steel cylindrical shell did not affect the load carrying capacity of the cylinder. Hence, it can be said that for a relatively thick cylinder with circumferential crack along the flanges, change in crack length has little or no significant effect on the buckling behavior of the cylinder. It looked like a further numerical investigation would be appropriate in order to gain a wider knowledge into the buckling behavior of a cylinder model generated with integral top and bottom flanges having circumferential crack along the flange.

ACKNOWLEDGEMENTS

The author will like to acknowledge the financial support received from the Faculty of Engineering Technology, Universiti Teknikal Malaysia Melaka under the auspices of UTeM short terms funding.

REFERENCES

[1] Razak NAA, Ng SS. Investigation of Effects of MIG Welding on Corrosion Behaviour of AISI 1010 Carbon Steel. 2014.

[2] Charde N. Characterization of spot weld growth on dissimilar joints with different thicknesses. Journal of Mechanical Engineering and Sciences. 2012;2:172-80.

[3] Daud R, Ariffin A, Abdullah S. Validation of crack interaction limit model for parallel edge cracks using two-dimensional finite element analysis. International Journal of Automotive and Mechanical Engineering. 2013;7:993.

[4] Simitses GJ. Buckling and postbuckling of imperfect cylindrical shells: a review. Applied Mechanics Reviews. 1986;39:1517-24.

[5] Estekanchi H, Vafai A. On the buckling of cylindrical shells with through cracks under axial load. Thin-walled structures. 1999;35:255-74.

[6] Ayari F, Zghal A, Bayraktar E. Numerical Study of Cracked Titanium Shell under Compression. Advanced Materials Research: Trans Tech Publ; 2011. p. 490-5.

[7] Jahromi BH, Vaziri A. Instability of cylindrical shells with single and multiple cracks under axial compression. Thin-Walled Structures. 2012;54:35-43.

[8] Javidruzi M, Vafai A, Chen J, Chilton J. Vibration, buckling and dynamic stability of cracked cylindrical shells. Thin-Walled Structures. 2004;42:79-99.

[9] Kim Y. Buckling of a cracked cylindrical shell reinforced with an elastic liner: Citeseer; 2011.

[10] Kim Y, Haghpanah B, Ghosh R, Ali H, Hamouda A, Vaziri A. Instability of a cracked cylindrical shell reinforced by an elastic liner. Thin-walled structures. 2013;70:39-48.
[11] Vaziri A, Estekanchi H. Buckling of cracked cylindrical thin shells under combined internal pressure and axial compression. Thin-Walled Structures. 2006;44:141-51.
[12] Kabir M, Nazari A. Numerical study on reinforcing of thin walled cracked metal cylindrical columns using FRP patch. Scientia Iranica Transaction A, Civil Engineering. 2010;17:407.
[13] Vafaei A, Estekanchi H. A prologue to the buckling analysis of cracked shells. 1996.
[14] Shariati M, Sedighi M, Saemi J, Eipakchi H, Allahbakhsh H. Numerical and experimental investigation on ultimate strength of cracked cylindrical shells subjected to combined loading. Mechanika. 2010;4:12-9.
[15] Starnes JH, Rose CA. Buckling and stable tearing responses of unstiffened aluminum shells with long cracks. The 39th AIAA/ASME/ASCE/AHS/ASC Structures, Structural Dynamics and Materials Conference and Exhibit1998. p. 20-3.
[16] Starnes JH, Rose CA. Nonlinear response of thin cylindrical shells with longitudinal cracks and subjected to internal pressure and axial compression loads. NASA Conference Publication: NASA; 1998. p. 197-208.
[17] Vaziri A, Nayeb-Hashemi H, Estekanchi H. Dynamic response of cracked cylindrical shells with internal pressure. ASME 2002 International Mechanical Engineering Congress and Exposition: American Society of Mechanical Engineers; 2002. p. 257-65.
[18] Vaziri A, Nayeb-Hashemi H, Estekanchi H. Buckling of the composite cracked cylindrical shells subjected to axial load. ASME 2003 International Mechanical Engineering Congress and Exposition: American Society of Mechanical Engineers; 2003. p. 87-93.
[19] Vaziri A. On the buckling of cracked composite cylindrical shells under axial compression. Composite structures. 2007;80:152-8.
[20] Allahbakhsh H, Shariati M. Buckling of Cracked laminated composite cylindrical shells subjected to combined loading. Applied Composite Materials. 2013;20:761-72.
[21] Allahbakhsh H, Shariati M. Instability of cracked CFRP composite cylindrical shells under combined loading. Thin-Walled Structures. 2014;74:28-35.
[22] Hibbeler R. Mechanics of Materials. 9 ed: Prentice Hall, Upper Saddle River; 2013.
[23] EN B. 10002-1: Tensile testing of Metallic Materials, Part (1), Method of test at ambient temperature. British Standard Institute, London, UK. 2001.
[24] Ifayefunmi O. Buckling behavior of axially compressed cylindrical shells: Comparison of theoretical and experimental data. Thin-Walled Structures. 2016;98:558-64.
[25] Ifayefunmi O, Błachut J. The Effect of Shape, Thickness and Boundary Imperfections on Plastic Buckling of Cones. ASME 2011 30th International Conference on Ocean, Offshore and Arctic Engineering: American Society of Mechanical Engineers; 2011. p. 23-33.
[26] Ifayefunmi OF. Combined stability of conical shells: University of Liverpool; 2011.